IEEE Access
Multidisciplinary | Rapid Review | Open Access Journal

Received January 22, 2019, accepted February 12, 2019, date of publication February 21, 2019, date of current version April 15, 2019.

Digital Object Identifier 10.1109/ACCESS.2019.2899915

A Bi-Layer Multi-Time Coordination Method for Optimal Generation and Reserve Schedule and Dispatch of a Grid-Connected Microgrid

XIA LEI[1], (Member, IEEE), TAO HUANG[1,2], (Member, IEEE), YI YANG[3], YONG FANG[1], AND PENG WANG[4], (Fellow, IEEE)

[1]School of Electrical Engineering and Electronic Information, Xihua University, Chengdu 610039, China
[2]Department of Energy, Politecnico di Torino, 10129 Torino, Italy
[3]Bazhong Electrical Company, Bazhong 636600, China
[4]Electrical and Electronic Engineering School, Nanyang Technological University, Singapore 639798

Corresponding authors: Xia Lei (snow_lei246@mail.xhu.edu.cn) and Tao Huang (tao.huang@polito.it)

This work was supported in part by the Chunhui Project of Ministry of Education under Grant Z2016145, in part by the National Natural Science Foundation of China under Grant 51877181, in part by the Major Cultivation Project of Sichuan Education Department under Grant 18CZ0018, and in part by the Key Project of Science and Technology Department of Sichuan Province under Grant 2019YFG0153.

ABSTRACT With the integration of more microgrids in distribution networks, its optimal autonomous operation becomes more important to reduce its operating cost and its influence on the main grid. This paper proposes a bi-layer multi-time coordination method for optimal generation and reserve schedule and dispatch of a grid-connected microgrid to reduce the impact of uncertainties of renewable sources, loads, and random component failures on power balance, operating costs, and system reliability. The reserve is refined into positive and negative reserves related to power shortage and power surplus. In the days ahead schedule layer, generating units are committed, and relaxed bidirectional reserve boundaries are predicted for the next day. In the real-time dispatch layer, generation output is dynamically adjusted and the reserve is dispatched using a successive approximation based on real-time data. A test microgrid is analyzed to illustrate the effectiveness of the proposed approach.

INDEX TERMS Generation dispatch, reserve allocation, microgrid, multi-time scale framework, operational performance.

NOMENCLATURE

Acronym:

DG	Distributed generator
PV	Photovoltaic
WT	Wind turbine
BS	Battery storage
SOC	State of Charge
MG	Microgrid
PNU	Power not used
LNS	Load not supplied

Indices:

T	Schedule time period (subscript)
t	Dispatch time period (subscript)
$t+/t-$	The subscript $t+$ represents the parameters relative to positive reserve;$t-$ represents negative reserve
i	Component index or load type index(subscript)
k	Fault scenario index(subscript)

Parameters:

N	Adjustment number of reserve
h	Adjustment step of reserve
u^{Tie}	$\begin{cases}1: & \text{power from main grid to MG}\\ 0: & \text{power from MG to main grid}\end{cases}$
u^{DG}	$\begin{cases}1: & \text{DGcommitted}\\ 0: & \text{DG shut down}\end{cases}$
$\beta_1/\beta_2/\beta_3$	Penalty cost coefficients for deviation of voltage, SOC limit and power plan
η^{Ch}/η^{Dis}	Charge and discharge efficiencies of BS

The associate editor coordinating the review of this manuscript and approving it for publication was Tiago Cruz.

$\xi^L/\xi^{WT}/\xi^{PV}$	Power prediction deviation of load, WT and PV
$\eta_k^{Ch}/\eta_k^{Dis}/\eta_k^{PV}$	Forecast error probabilities of load, WT and PV in scenario k
F^{out}	The forced outage rate of the committed units
ΔT	Duration of period T
Δt	Duration of period t
c^{M}	Maintenance price of MG
$c^{\text{P}}/c^{\text{S}}$	Power purchase price from grid and sale price to grid
$c^{\text{Rg}}/c^{\text{Rbat}}$	Ramp loss coefficients of dispatchable DG and BS
c^{LNS}	Compensation price of LNS
c^{PNU}	Penalty price of PNU
P^{out}	Power that should have been provided by outage DGs
$\overline{S^{\text{Bat}}}/\underline{S^{\text{Bat}}}$	Upper and lower limit of SOC
$\overline{P^{\text{Tie}}}/\underline{P^{\text{Tie}}}$	Upper and lower power limit of tie-line between MG and main grid
V^{R}	Rated voltage of MG
$r^{\text{Up}}/r^{\text{Up,Bat}}$	Ramp up rate of controllable DG and BS
$r^{\text{Down}}/r^{\text{Down,Bat}}$	Ramp down rate of controllable DG and BS
E^{Bat}	Rated capacity of BS
R^{out}	Available reserve that would have been provided by outage DGs
E^{LNS}	Required threshold for LNS (RTLNS)
E^{PNU}	Required threshold for PNU (RTPNU)
Variables:	
α_k	Probability of scenario k
V^{min}	Minimum bus voltage of MG
S^{Bat}	SOC of BS
C^{S}	Total operational cost of MG in schedule layer
C^{OM}	Operation and maintenance cost
C^{Vd}	Voltage deviation cost
C^{Bat}	SOC violation cost
C^{Fuel}	Fuel cost of conventional DGs
C^{M}	PMaintenance cost of MG
C^{Tie}	Power exchange cost with the main grid
C^{D}	Total cost in dispatch layer
C^{PF}	Additional cost for the power deviation from the scheduled power
C^{R}	Cost of power regulation
C^{Risk}	Risk cost
$C^{\text{LNS}}/C^{\text{PNU}}$	Cost of LNS and PNU
$P^{\text{Ch}}/P^{\text{Dis}}$	Charging and discharging power of BS
$P^{\text{DG}}/P^{\text{Bat}}$	Power output of the controllable DG and BS
P^{Tie}	Power exchange between MG and the main grid
$P^{\text{L}}/P^{\text{WT}}/P^{\text{PV}}$	Power of load, WT and PV
P^{Gap}	Power discrepancy between the total load and the total generation
P^{Loss}	Loss load within RTLNS constraint
P^{LW}	Power not supplied or not used
ΔP^{Tie}	Regulated power between MG and the main grid
$\overline{P^{\text{DG}}}/\underline{P^{\text{DG}}}$	Upper and lower output of controllable DG
$\overline{P^{\text{Bat}}}/\underline{P^{\text{Bat}}}$	Upper and lower output power of BS
$\overline{R^{\text{d}}}/\underline{R^{\text{d}}}$	Upper and lower limit of reserve
R^{d}	Total reserve of MG
$R^{\text{DG}}/R^{\text{Bat}}$	Reserve provided by the controllable DGs and BS
R^{h}	Reserve adjustment factor

I. INTRODUCTION

As an aggregate with renewables and DGs, MGs with optimal autonomous operation can reduce the impact of the intrinsic randomness and intermittency of renewables on the main grid [1]–[3]. Nevertheless, accompanied by its flexibility, the MG also brings disturbances to the main grid due to the uncertainties of being a load or a source with time. Therefore, with integration of more MGs in distribution networks, the optimal autonomous operation of a MG becomes increasingly important for improving its own controllability, economics, sustainability and reliability and reducing its influence on the main grid [4]–[9].

The major challenge for the optimal MG operation strategy is to combat the uncertainties from different aspects [10]. Two aspects that solve the problem include modeling of system behaviors under uncertainties and designing a dispatch regime to prepare the system withstand these uncertainties. Methods of probabilities including Monte Carlo simulation [11]–[15] and stochastic programming [16]–[18] have been used to derive overall control strategies; however, results obtained from these methods could be highly dependent on assumptions for stochastic decision variables, their correlations and the confidence levels. The computational burden of using these methods is commonly huge and sometimes intractable, which may limit practical and real-time applications. A robust optimization was proposed to optimize the control strategies of the MG with a certain measure of robustness against uncertainties [8], [19], [20]. Nevertheless, a robust optimization based on worst cases may sometimes overpessimistically emphasize the problems so that the feasible region is reduced and resulting to an ineffective solution.

On the other hand, for the dispatching framework, a multi-time scale coordinated dispatch that is based on a rolling horizon for longer-time-ahead schedule and shorter-time-ahead adjustment has been verified as an effective strategy to tackle uncertainties in reality [21]. For example, [22], [23] used the framework to solve the randomness of renewables. Bao *et al.* [24], [25] presented a multi- time-scale coordinated scheduling solution of a grid-connected MG with multiple energy types for both the cooling and electricity demands. Moreover, an online moving horizon optimization strategy was proposed based on the model predictive control for an isolated power system in [26]. Three or more

stages coordination strategy for the renewable connected grid has also been studied [27], [28]. Li *et al.* [29] discussed a dispatch within dynamic time-scale adjustment. As the multi-time-scale coordinated dispatch considered both the scheduled and the real-time operation of the system under some uncertainties, examples of such framework are not rare in reality. The result of the multi-time-scale dispatch can balance the generation and demand for as much as possible by changing the generators' output, yet the reliability can only be guaranteed by the reserve inside the grid (MG). However, the reserve problem is not fully covered in most of the studies, which may lead to a decrease of security and reliability of MG. Mohan *et al.* [30] thought that if possible variations in the energy schedule could be estimated in the planning horizon, the required reserve could be dispatched in real/quasi-real-time mode based on it.

The reserve configuration is viewed as an important issue both for a reliable and economic operation of an islanded MG [31], as well as for resilience improvement of a sudden change from the grid-connected mode to the islanded one [7], [8], [32]. As the main grid can provide infinite supply or demand to a MG, conventional research on the grid-connected MG has been focused on its economic operation without explicitly considering its reserve. However, with the increasing MG penetration in the distribution network, the main grid faces the challenge of loss of the ''infinite'' feature of reserve for all grid-connected MGs. Moreover, it is difficult for an Independent System Operator (ISO) to obtain the accurate reserve demands of each grid-connected MG. Therefore, it is important for a MG operator to sufficiently utilize the local resources as reserve. The configuration of the reserve in the main grid with renewable sources has been sufficiently discussed in many literatures, such as [33] and [34], yet the method is unfit to be directly used in the MGs due to the different strictness on the reserve requirement. For example, security constraints in the main grid must be satisfied so that the operational cost will increase, whereas some limits could be relaxed in the MG with support of the main grid. As a consequence, the operator of the grid-connected MGs only needs to rationally configure and use the available reserve sources inside their system (such as conventional units and BS [35] etc.), rather than strictly follow the same criterion used by the main grid. In [30], sensitivity analysis is too complicated to be used to estimate reserve in a grid-connected MG.

In summary, the multi-time-scale coordinated dispatch provides a framework to balance the power in a MG with renewables, while the reserve can provide a certain degree of reliability to the operation of the MG with uncertain factors. However, how to incorporate the reserve configuration into a multi-time-scale coordinated dispatch is seldom discussed.

The main contributions of this paper include the following:

- A bi-layer coordinated generation and reserve schedule method is proposed to for a grid-connected MG in a multi-time-scale framework to reduce the impact of uncertainties on power balance, operating costs and system reliability.
- A relaxed reserve configuration model with bidirectional boundaries constraints is proposed to cope with the uncertainties in the optimal scheduling problem.
- A simple iterative method is proposed to quickly acquire an accurate reserve configuration through a successive approximation within the bidirectional boundaries for real-time applications.
- Three probability indicators are proposed to indicate the operational performances of the grid-connected MG.

The paper is organized as follows. Section II presents the dynamic bi-layer coordinated generation and reserve schedule and dispatch model. A flow chart of calculating the model is depicted. Section III presents the simulation results and analysis. Finally, section IV provides the conclusions.

II. DYNAMIC BI-LAYER COORDINATED GENERATION AND RESERVE SCHEDULE AND DISPATCH

The dynamic dispatch, which coordinates generation of DGs over multiple time scales, has been verified to improve suitability for considering more system operating requirements than those of the static dispatch for independent periods. Modeling and formulation of a dynamic bi-layer generation and reserve schedule and dispatch are presented in this section. In upper layer, a day-ahead hourly schedule is determined for each time period T based on the forecasting data of the next 24 hours. The units are committed based on the minimum operating costs. Forecasting errors of renewables and loads may be significant 24 hours in advance, creating difficulty in calculating the accurate reserve for each time period T of the following day. Therefore the bidirectional reserve boundaries are determined based on the probability models of uncertainties, ramp rates of controllable units, RTLNS and RTPNU etc. in the schedule layer. In lower layer, a schedule period of T is divided into 5-minute dispatch periods and the scheduled generation is adjusted every 5 minute to follow the fluctuation of PV, WT, load and random generator outages. The reserve is determined through a successive approximation in the dispatch layer within the reserve boundaries.

A. UNIT COMMITMENT AND RESERVE BOUNDARIES IN SCHEDULE LAYER

The optimization model of available generation is developed daily ahead for a MG, and then bidirectional reserve boundaries are determined in this.

1) UNIT COMMITMENT

Unit commitment and generation schedule in the schedule layer for next 24 hours aims to minimize the total operational cost C^{S} of MG with considering power supply quality, the impact on the main grid, the schedulability of BS and system operational constraints. The objective function is expressed as follows:

$$\min C^{\mathrm{S}} = \sum_{T} (C_T^{\mathrm{OM}} + C_T^{\mathrm{Vd}}) + C^{\mathrm{Bat}} \tag{1}$$

where

$$C_T^{\mathrm{OM}} = \sum_i (C_{i,T}^{\mathrm{Fuel}} + C_{i,T}^{\mathrm{M}}) + C_T^{\mathrm{Tie}} \tag{2}$$

and $C_{i,T}^{\mathrm{Fuel}}$ is the fuel cost of conventional DG i, which is expressed by a quadratic function.

$$C_{i,T}^{\mathrm{M}} = c_i^{\mathrm{M}} P_{i,T}^{\mathrm{DG}} \tag{3}$$

$$C_T^{\mathrm{Tie}} = u_T^{\mathrm{Tie}} c_T^{\mathrm{P}} P_T^{\mathrm{Tie}} - (1 - u_T^{\mathrm{Tie}}) c_T^{\mathrm{S}} P_T^{\mathrm{Tie}} \tag{4}$$

The C_T^{Vd} set in the objective function is to improve the power supply quality of the customer as one of the schedule targets. The difference between $V_T^{\min}$ and V^{R} is used to calculate the voltage deviation cost.

$$C_T^{\mathrm{Vd}} = \beta_1 \left| 1 - V_T^{\min} / V^{\mathrm{R}} \right| \tag{5}$$

To ensure schedulability of BS on the next day, its SOC at the beginning of the day is assumed to as equal to that at the day-end [36].The penalty cost C^{Bat} for an insufficient SOC is expressed by (6).

$$C^{\mathrm{Bat}} = \beta_2 \left| \sum_{T, P_T^{\mathrm{Bat}} < 0} \eta^{\mathrm{Ch}} P_T^{\mathrm{Ch}} + \sum_{T, P_T^{\mathrm{Bat}} > 0} (P_T^{\mathrm{Dis}} / \eta^{\mathrm{Dis}}) \right| \tag{6}$$

where $\sum_{T, P_T^{\mathrm{Bat}} < 0} \eta^{\mathrm{Ch}} P_T^{\mathrm{Ch}}$ is the sum of charge power(negative) and $\sum_{T, P_T^{\mathrm{Bat}} > 0} (P_T^{\mathrm{Dis}} / \eta^{\mathrm{Dis}})$ is the sum of discharge power(positive) during the next day.

The objective function is subject to the following constraints:

The SOC constraint is expressed as

$$\begin{cases} \underline{S^{\mathrm{Bat}}} \le S_T^{\mathrm{Bat}} \le \overline{S^{\mathrm{Bat}}} \\ S_T^{\mathrm{Bat}} = S_{T-1}^{\mathrm{Bat}} - (\eta^{\mathrm{Ch}} P_T^{\mathrm{Ch}} + P_T^{\mathrm{Dis}} / \eta^{\mathrm{Dis}}) \Delta T / E^{\mathrm{Bat}} \end{cases} \tag{7}$$

where $\overline{S^{\mathrm{Bat}}} = 0.8$ and $\underline{S^{\mathrm{Bat}}} = 0.2$.

The power limits are described as

$$\begin{cases} \underline{P_{i,T}^{\mathrm{DG}}} \le P_{i,T}^{\mathrm{DG}} \le \overline{P_{i,T}^{\mathrm{DG}}} \\ \underline{P_T^{\mathrm{Tie}}} \le P_T^{\mathrm{Tie}} \le \overline{P_T^{\mathrm{Tie}}} \\ \underline{P_T^{\mathrm{Bat}}} \le P_T^{\mathrm{Bat}} \le \overline{P_T^{\mathrm{Bat}}} \end{cases} \tag{8}$$

where

$$\begin{cases} \overline{P_{i,T}^{\mathrm{DG}}} = \min(P_{i,T-1}^{\mathrm{DG}} + r_i^{\mathrm{Up}} \Delta T, \overline{P_i^{\mathrm{DG}}}) \\ \underline{P_{i,T}^{\mathrm{DG}}} = \max(P_{i,T-1}^{\mathrm{DG}} - r_i^{\mathrm{Down}} \Delta T, \underline{P_i^{\mathrm{DG}}}) \end{cases} \tag{9}$$

$$\begin{cases} \overline{P_T^{\mathrm{Bat}}} = \min(\overline{P^{\mathrm{Bat}}}, (S_{T-1}^{\mathrm{Bat}} - \underline{S^{\mathrm{Bat}}}) E^{\mathrm{Bat}} \eta^{\mathrm{Dis}} / \Delta T, \\ \qquad P_{T-1}^{\mathrm{Bat}} + r^{\mathrm{Up,Bat}} \Delta T) \\ \underline{P_T^{\mathrm{Bat}}} = \max(\underline{P^{\mathrm{Bat}}}, (\overline{S^{\mathrm{Bat}}} - S_{T-1}^{\mathrm{Bat}}) E^{\mathrm{Bat}} / (\eta^{\mathrm{Ch}} \Delta T), \\ \qquad P_{T-1}^{\mathrm{Bat}} - r^{\mathrm{Down,Bat}} \Delta T) \end{cases} \tag{10}$$

The ramp rate constraints of schedulable DG and BS are

$$\begin{cases} -r_i^{\mathrm{Down}} \Delta T \le P_{i,T}^{\mathrm{DG}} - P_{i,T-1}^{\mathrm{DG}} \le r_i^{\mathrm{Up}} \Delta T \\ -r^{\mathrm{Down,Bat}} \Delta T \le P_T^{\mathrm{Bat}} - P_{T-1}^{\mathrm{Bat}} \le r^{\mathrm{Up,Bat}} \Delta T \end{cases} \tag{11}$$

The power balance constraint of MG is given by

$$\sum_i P_{i,T}^{\mathrm{WT}} + \sum_i P_{i,T}^{\mathrm{PV}} + \sum_i P_{i,T}^{\mathrm{DG}} + P_T^{\mathrm{Bat}} + P_T^{\mathrm{Tie}} = \sum_i P_{i,T}^{\mathrm{L}} \tag{12}$$

2) BIDIRECTIONAL RESERVE BOUNDARIES DETERMINATION

The reserve boundaries are determined on unit commitment to reduce the risks of uncertainties. Based on the mismatch between the total generation and the total load, the reserve can be categorized into the positive and negative reserves. The positive reserve is supplied to compensate power shortages, whereas negative reserve is used to reduce power surplus. For convenience in the dynamic adjustment of reserves in dispatch layer, the boundaries of positive and negative reserves are estimated in shorter dispatch time periods (t) of the next day. Power output in t is derived by linearization of the optimized power in T.

The positive reserve boundary is as

$$\underline{R_{t+}^{\mathrm{d}}} \le R_{t+}^{\mathrm{d}} \le \overline{R_{t+}^{\mathrm{d}}} \tag{13}$$

where the upper limit of positive reserve $\overline{R_{t+}^{\mathrm{d}}}$ described as (14) is determined by the reserve provided by committed DGs and BS in t. The reserve provided by DG i(/BS) in $tR_{i,t+}^{\mathrm{DG}}$ as (15) (R_{t+}^{Bat} as (16)) is the lower between the ramp up power during t and the remaining capacity of DG i(/BS).

$$\overline{R_{t+}^{\mathrm{d}}} = \sum_k \sum_i (1 - \alpha_k) (u_{i,T}^{\mathrm{DG}} R_{i,t+}^{\mathrm{DG}} + R_{t+}^{\mathrm{Bat}}) \quad (t \in T) \tag{14}$$

$$R_{i,t+}^{\mathrm{DG}} = \min(r_i^{\mathrm{Up}} \Delta t, \overline{P_i^{\mathrm{DG}}} - P_{i,t}^{\mathrm{DG}}) \tag{15}$$

$$R_{t+}^{\mathrm{Bat}} = \min(r^{\mathrm{Up,Bat}} \Delta t, \overline{P^{\mathrm{Bat}}} - P_t^{\mathrm{Bat}}) \tag{16}$$

where α_k can be obtained by multiplying the forecast error probability and outage rate as expressed by [37]

$$\alpha_k = \prod_i \eta_{i,k}^{\mathrm{L}} \prod_i \eta_{i,k}^{\mathrm{WT}} \prod_i \eta_{i,k}^{\mathrm{PV}} \prod_i F_{i,k}^{\mathrm{out}} \tag{17}$$

where $\eta_k^{\mathrm{L}}, \eta_k^{\mathrm{WT}}$ and η_k^{PV} follow a normal distribution $N(0, \delta^2)$ [38].

The R_{t+}^{d} is obtained by power shortage and reserve which should have been provided by outage DGs except for loss load (related to RTLNS). It is formulated as

$$\underline{R_{t+}^{\mathrm{d}}} = \sum_k (1 - \alpha_k) (P_{k,t+}^{\mathrm{Gap}} + \sum_i R_{i,k,t+}^{\mathrm{out}}) - \sum_i E_{i,t}^{\mathrm{LNS}} \tag{18}$$

where

$$P_{k,t+}^{\mathrm{Gap}} = \sum_i \xi_{i,k}^{\mathrm{L}} - \sum_i \xi_{i,k}^{\mathrm{WT}} - \sum_i \xi_{i,k}^{\mathrm{PV}} + \sum_i P_{i,k,t+}^{\mathrm{out}} \tag{19}$$

The negative reserve boundary is as

$$\underline{R_{t-}^{\mathrm{d}}} \le R_{t-}^{\mathrm{d}} \le \overline{R_{t-}^{\mathrm{d}}} \tag{20}$$

The $\underline{R_{t-}^{\mathrm{d}}}$ and $\overline{R_{t-}^{\mathrm{d}}}$ are derived as $\underline{R_{t+}^{\mathrm{d}}}$ and $\overline{R_{t+}^{\mathrm{d}}}$. Nevertheless, the expressions are related to the ramp down rate of DGs and

BS and RTPNU.

$$\overline{R^{\mathrm{d}}_{t-}} = \sum_k \sum_i (1-\alpha_k)\,(u^{\mathrm{DG}}_{i,T} R^{\mathrm{DG}}_{i,t-} + R^{\mathrm{Bat}}_{t-}) \quad (t \in T) \tag{21}$$

$$R_{i,t-} = \min(r^{\mathrm{Down}}_i \Delta t,\, P^{\mathrm{DG}}_{i,t} - \underline{P^{\mathrm{DG}}_i}) \tag{22}$$

$$R^{\mathrm{Bat}}_{t-} = \min(r^{\mathrm{Down,Bat}} \Delta t,\, P^{\mathrm{Bat}}_t - \underline{P^{\mathrm{Bat}}}) \tag{23}$$

$$\underline{R^{\mathrm{d}}_{t-}} = \sum_k (1-\alpha_k)\,(P^{\mathrm{Gap}}_{k,t-} + \sum_i R^{\mathrm{out}}_{i,k,t-}) - E^{\mathrm{PNU}}_t \tag{24}$$

$$P^{\mathrm{Gap}}_{k,t-} = \sum_i \xi^{\mathrm{WT}}_{i,k} + \sum_i \xi^{\mathrm{PV}}_{i,k} - \sum_i \xi^{\mathrm{L}}_{i,k} - \sum_i P^{\mathrm{out}}_{i,k,t-} \tag{25}$$

B. POWER AND RESERVE ALLOCATION IN DISPATCH LAYER

1) POWER DISPATCH

The objective function in dispatch layer for each operating period of 5 minutes aims to minimize the total dispatch cost and is expressed as follows.

$$\min C^{\mathrm{D}}_t = C^{\mathrm{PF}}_t + C^{\mathrm{R}}_t + C^{\mathrm{Risk}}_t \tag{26}$$

To guarantee that the power of controllable units in dispatch layer follows closely the generation schedule of the upper layer to minimize operational cost, the cost C^{PF}_t for power deviation from the generation schedule is expressed as

$$C^{\mathrm{PF}}_t = \beta_3[\sum_i (P^{\mathrm{DG}}_{i,t} - P^{\mathrm{DG}}_{i,T})^2 + (P^{\mathrm{Bat}}_t - P^{\mathrm{Bat}}_T)^2 + (P^{\mathrm{Tie}}_t - P^{\mathrm{Tie}}_T)^2] \quad (t \in T) \tag{27}$$

The cost of power regulation C^{R}_t includes the adjustment cost of either the positive or the negative reserve and tie-line with the grid. It can be expressed as follows.

$$C^{\mathrm{R}}_t = \sum_i u^{\mathrm{DG}}_{i,t} c^{\mathrm{Rg}}_i R^{\mathrm{DG}}_{i,t+(t-)} + c^{\mathrm{Rbat}} R^{\mathrm{Bat}}_{t+(t-)} + u^{\mathrm{Tie}}_t c^{\mathrm{P}}_t \Delta P^{\mathrm{Tie}}_t - (1-u^{\mathrm{Tie}}_t) c^{\mathrm{S}}_t \Delta P^{\mathrm{Tie}}_t \tag{28}$$

To decrease the risk of load shedding and resources abandoning owing to insufficient reserve, risk cost C^{Risk}_t is set equal to load shedding compensation C^{LNS}_t or penalty of PNU C^{PNU}_t.

$$C^{\mathrm{PNU}}_t = c^{\mathrm{PNU}}_t P^{\mathrm{LW}}_t \tag{29}$$

$$C^{\mathrm{LNS}}_t = \sum_i c^{\mathrm{LNS}}_{i,t} P^{\mathrm{Loss}}_{i,t} \tag{30}$$

where

$$P^{\mathrm{Loss}}_{i,t} = \left(E^{\mathrm{LNS}}_{i,t} / \sum_i E^{\mathrm{LNS}}_{i,t} \right) P^{\mathrm{LW}}_t \tag{31}$$

$$P^{\mathrm{LW}}_t = abs(P^{\mathrm{Gap}}_t) - R^{\mathrm{d}}_{t+(t-)} \tag{32}$$

$$P^{\mathrm{Gap}}_t = \sum_i (P^{\mathrm{L}}_{i,t} \pm \xi^{\mathrm{L}}_{i,t}) - \sum_i P^{\mathrm{DG}}_{i,t} - P^{\mathrm{Bat}}_t - P^{\mathrm{Tie}}_t - \sum_i (P^{\mathrm{WT}}_i \pm \xi^{\mathrm{WT}}_{i,t}) - \sum_i (P^{\mathrm{PV}}_{i,t} \pm \xi^{\mathrm{PV}}_{i,t}) \tag{33}$$

2) RESERVE ALLOCATION WITHIN THE BOUNDARIES

The optimal reserve allocation is important to the security of MG, and the mathematical optimization method of reserve configuration is normally complicated and slow. Rapid calculation in dispatch layer is necessary due to the short dispatch time interval. The total reserve $R^{\mathrm{d}}_{t+(t-)}$ is determined by dynamic regulation within the boundaries estimated in schedule layer, and successive approximation is utilized to dynamically regulate reserve effectively and rapidly in this work. The reserve is adjusted through a positive or negative reserve adjustment factor $R^{\mathrm{h}}_{t+(t-)}$, which is related with adjustment number N. The larger is the N, the more accurate is the adjustment of reserve, but with slower calculation.

$$R^{\mathrm{h}}_{t+(t-)} = h \frac{\overline{R^{\mathrm{d}}_{t+(t-)}} - \underline{R^{\mathrm{d}}_{t+(t-)}}}{N} \quad (0 \le h \le N) \tag{34}$$

Thus, the reserve increases with successive increase of adjustment step h. The $R^{\mathrm{d}}_{t+(t-)}$ is regulated by

$$R^{\mathrm{d}}_{t+(t-)} = R^{\mathrm{d}}_{t+(t-)} + R^{\mathrm{h}}_{t+(t-)} \tag{35}$$

The constraints of the dispatch layer include upper and lower powers of controllable units and BS, power balance equations and reserve limits, which are expressed as follows.

$$\begin{cases} \underline{P^{\mathrm{G}}_{i,t}} \le P^{\mathrm{G}}_{i,t} \le \overline{P^{\mathrm{G}}_{i,t}} \\ \underline{P^{\mathrm{Tie}}_t} \le P^{\mathrm{Tie}}_t \le \overline{P^{\mathrm{Tie}}_t} \\ \underline{P^{\mathrm{Bat}}_t} \le P^{\mathrm{Bat}}_t \le \overline{P^{\mathrm{Bat}}_t} \end{cases} \tag{36}$$

$$\sum_i (P^{\mathrm{WT}}_{i,t} \pm \xi^{\mathrm{WT}}_{i,t}) + \sum_i (P^{\mathrm{PV}}_{i,t} \pm \xi^{\mathrm{PV}}_{i,t}) + \sum_i u^{\mathrm{DG}}_{i,t} P^{\mathrm{G}}_{i,t} + P^{\mathrm{Bat}}_t + P^{\mathrm{Tie}}_t = \sum_i (P^{\mathrm{L}}_{i,t} \pm \xi^{\mathrm{L}}_{i,t}) \tag{37}$$

where $\underline{P^{\mathrm{G}}_{i,t}}$, $\overline{P^{\mathrm{G}}_{i,t}}$, $\underline{P^{\mathrm{Bat}}_t}$ and $\overline{P^{\mathrm{Bat}}_t}$ are got as formulation (9) and (10).

C. PROCEDURE OF DYNAMIC BI-LAYER GENERATION AND RESERVE SCHEDULE AND DISPATCH

To solve the bi-layer coordinated dispatch for MG energy management, the particle swarm optimization (PSO) algorithm is employed in this paper [39], [40]. The power outputs of uncontrollable units, exchange power of tie-line and reserve are decision variables.

Figure 1 shows the calculation flow of the bi-layer coordinated dispatch of the MG. The flow chart includes three main modules: schedule layer, dispatch layer and self-adaption module. The self-adaption module is described in Fig. 2.

The calculation flow is described as follows:

Step 1: In the schedule layer, units are committed to economic operation based on renewables and load forecasting during each period of times T for the next day.

Step 2: The positive and negative reserve boundaries are assessed in each time period T (decomposed linearly in t) for the next day considering power forecasting errors and DG outage rate.

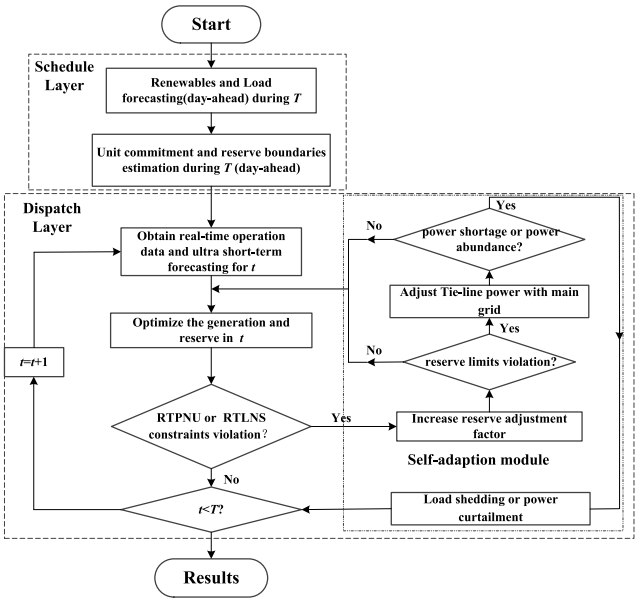

FIGURE 1. Flowchart of the MG bi-layer coordination dispatch.

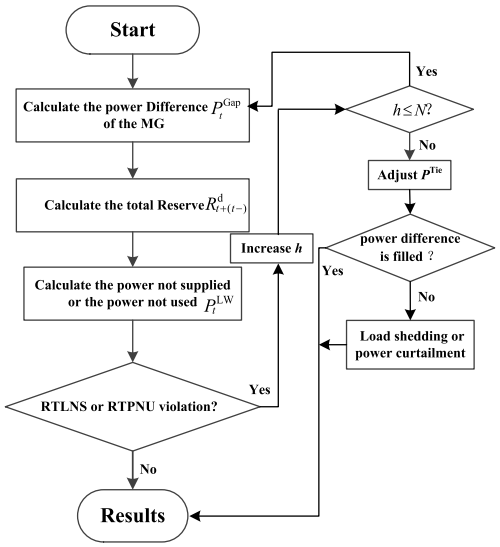

FIGURE 2. Flowchart of the reserve allocation.

Step 3: In the dispatch layer, based on the real-time operation data and ultra-short-term forecasting in t, unit optimal output is regulated to minimize operational cost, risk cost, and power adjusting cost.

Step 4: The reserve requirement of the MG is calculated.

Step 5: Is RTNUP or RTLNS violated? If the answer is yes, the reserve is adjusted in self-adaption module (described in detail in Fig. 2), else proceed to the next step.

Step 6: Is $t < T$? If no, then the calculation procedure ends, else $t = t + 1$ and then return to step 3.

D. ADDITIONAL PERFORMANCE INDICES

f is used to represent prediction error of power, which is defined as the ratio of the standard deviation δ of forecast error to the predicted power P.

$$f = \delta / P \tag{38}$$

Three performance indices are defined to describe the influence of uncertainties on operation of both MG and the main grid. Fluctuation of tie-line power probability (FOPP) indicates the influence of MG on operation of the main grid. Load not supplied probability (LNSP) and power not used probability (PNUP) indicate the ability of the load supplied and the utilization efficiency of renewables. Three indices are defined as

$$FOPP = \sqrt{\sum_{t=1}^{T}(P_t^{\mathrm{Tie}} - P_T^{\mathrm{Tie}})^2} \Big/ \sqrt{\sum_{t=1}^{T}(P_t^{\mathrm{Tie}})^2} \quad (t \in T) \tag{39}$$

$$LNSP = \sum_{t=1}^{T}\sum_{i}(E_{i,t}^{\mathrm{LNS}} \Big/ \sum_{i} E_{i,t}^{\mathrm{LNS}})P_t^{\mathrm{LW}} \Big/ \sum_{t=1}^{T}\sum_{i} P_{i,t}^{\mathrm{L}} \tag{40}$$

$$PNUP = \sum_{t=1}^{T} P_t^{\mathrm{LW}} \Big/ \sum_{t=1}^{T}\sum_{i} P_{i,t}^{\mathrm{L}} \tag{41}$$

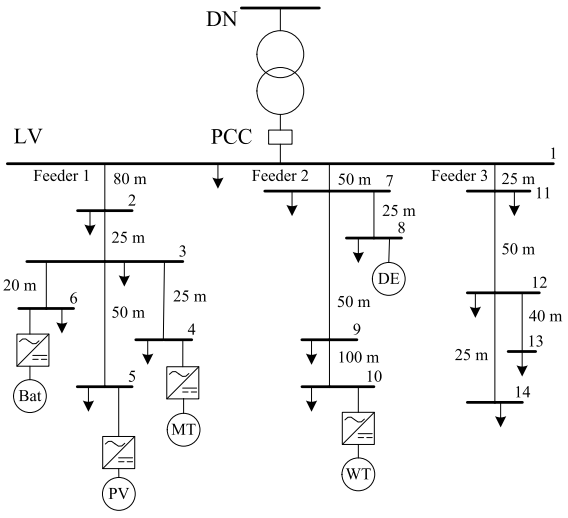

FIGURE 3. A typical MG with distributed renewables and battery storages.

III. CASE STUDIES

A. TEST SYSTEM

A modified low voltage (LV) MG based on the test system [23] is used to test the proposed models and techniques. Figure 3 shows the system, which consists of 14 buses, and is connected with the main grid through a static switch (SD) at a point of common coupling (PCC) that can isolate the MG from the main grid. The resistance is 0.64+j0.1 (ohms/km). The MG includes a 100kW PV unit and a 200kW WT unit, an 80kW MT (microturbine) and a 60kW DE (diesel engine), and a 200kW BS. The charge discharge cycle efficiency of the BS is 0.86, and the initial remaining power is 0.5.

TABLE 1. Parameters of DGs.

Type	Power(kW)		c^M	Ramp rate	Forced
	Min	Max	(￥/kW)	(kW/min)	outage rate
DE	3	60	0.0825	1	0.008
MT	5	80	0.0385	2	0.005
BS	-40	40	0.0275	6	0

The maximum transmission capacity between the MG and the main grid is 100 kW. The coefficients $\beta_1 = \beta_2 = 0.5$, $\beta_3 - 0.05$. Table 1 provides the parameters of the DG units in the MG, whereas the data of load nodes are shown in Table 2. One day is taken as an optimal operation cycle with 1h as an interval in the schedule layer. 5min is taken as an interval in the dispatch layer. The time-of-use price is used in the case (see Table 3).

TABLE 2. Data of load nodes in the MG.

Load node	Active power (kW)		Power factor	Load node	Active power (kW)		Power factor
	L1	L2			L1	L2	
1	0	30	0.9545	8	0	24	0.9781
2	12	32	0.9487	9	14	0	0.9417
3	24	0	0.9751	10	18	0	0.9654
4	0	40	0.9751	11	17.6	0	0.9772
5	20	0	0.9798	12	24	0	0.9487
6	30	0	0.9615	13	20	0	0.9728
7	24	48	0.9740	14	8	0	0.9790

TABLE 3. Purchase and sale prices for mg.

Type	Period	Price (￥/kWh)	
		Purchas	Sale
peak	10:00-15:00 ,18:00-21:00	0.83	0.65
plain	07:00-10:00,15:00-18:00 21:00-23:00	0.49	0.38
valley	23:00-the next day 07:00	0.17	0.13

Load is classified by household (L1) and industry (L2), for a fluctuation parameter f of 5%. The forecasting (dotted line) and real-time (solid line) data for L1 and L2 are provided in Figs. 4(a) and (b). In the figures, active power is expressed as per-unit value with forecasting peak load as base on the history data of wind speed and solar radiation intensity. PV and WT fluctuation parameters f are supposedly 10% and 5%, respectively. The forecasting (dotted line) and real-time (solid line) data for PV and WT units are provided in Figs. 4(c) and 4(d). The active power is expressed by the form of per-unit value with upper limit of output as the base value. The ratio of PNU to total prediction power of renewable units is 2×10^{-3}.

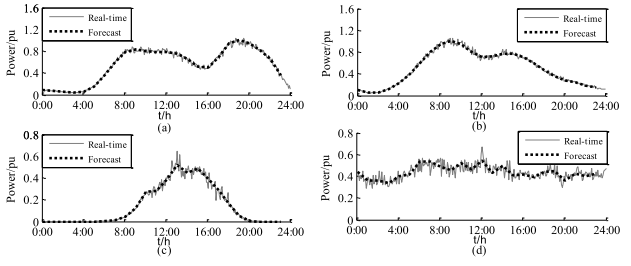

FIGURE 4. Forecast and real-time power of loads and renewable energy.

B. COMPARISON OF GENERATION OUTPUT AND COSTS BETWEEN DIFFERENT METHODS

The reserve capacity of is traditionally determined as the fixed proportion of system load (i.e. 5%-10%) or the biggest unit capacity in the MG. The 7% of the load is taken as the reserve capacity. Figure 5 shows optimal power outputs of the controllable units' in both schedule and dispatch layer with different reserve distribution strategies. It can be seen that the outputs of all controllable units in dispatch layer of both methods follow the economic power schedule well.

Table 4 shows the cost of the two reserve strategies. Because of the relaxed reserve configuration, the total operational cost of the proposed method is lower than the traditional method. The former is more economical. The fuel and maintenance costs of schedule layer of the proposed method are higher than those of the traditional method. The power adjustment cost of dispatch layer of the proposed method is higher than that of the traditional method. The results present that the proposed method utilizes more local resources. On the other hand, the exchange power cost with the main grid using the proposed method is less than that from the traditional method. The result illustrates that the impact of MG on the main grid in the proposed method is less than that in the traditional method, which is good for security of the main grid.

C. COMPARISON OF OPERATIONAL PERFORMANCES BETWEEN DIFFERENT METHODS

Table 5 and Fig. 6 show three operational indicators (FOPP, LNSP and PNUP) in different methods. The indicators obtained from the proposed approach are lower than those from the traditional method; therefore the proposed technique is more secure and reliable for MG and the main grid.

D. INFLUENCE OF PARAMETERS ON DISPATCH STRATEGY

1) INFLUENCE OF POWER FLUCTUATION

To analyze the impact of renewable DG units' f on the reserve capacity, the optimal scheduling results with different f are shown in Table 6. The results present that required reserve increases with the increase of f, at the same time that the operational cost of the schedule and the dispatch layers and the total operational cost increase. Moreover, the operational indicators FOPP, LNSP and PNUP also increase when the volatility parameters f increase.

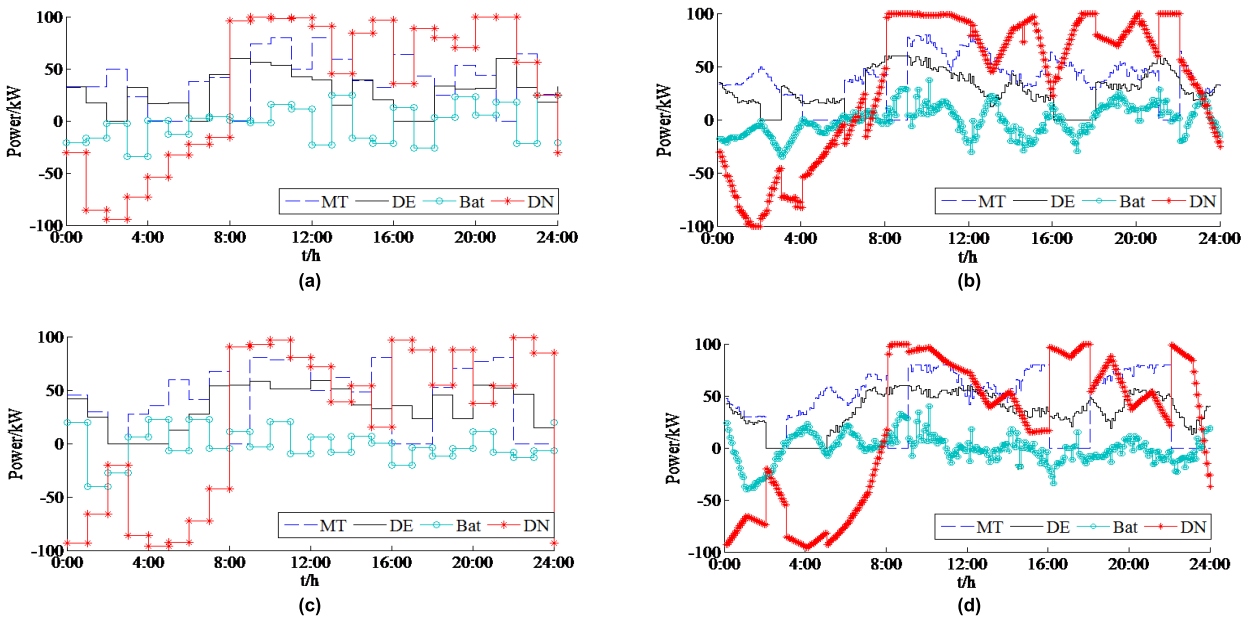

FIGURE 5. Outputs of controllable units with reserve distribution in traditional and proposed methods. (a) Schedule layer in traditional method. (b) Dispatch layer in traditional method. (c) Schedule layer in proposed method. (d) Dispatch layer in proposed method.

TABLE 4. The costs of MG with different models.

Different methods	Total operation cost (￥)	Schedule layer (￥)						Dispatch layer (￥)			
		Total cost	Operation and maintenance cost			Voltage deviation cost	SOC violation cost	Total cost	Power deviation cost	Power adjustment cost	Risk cost
			Fuel cost	Maintenance cost	Power exchange cost						
Traditional method	1947.23	1861.15	870.18	91.96	780.86	117.41	0.74	86.08	63.77	15.34	6.97
Proposed method	1890.53	1800.18	944.62	109.78	624.91	120.68	0.19	90.35	68.70	16.55	5.10

TABLE 5. Operational performances of mg.

Different methods	FOPP (10^{-4})	LNSP (10^{-4})	PNUP (10^{-4})
Traditional method	224.10	24.87	1.14
Proposed method	43.70	18.50	0.08

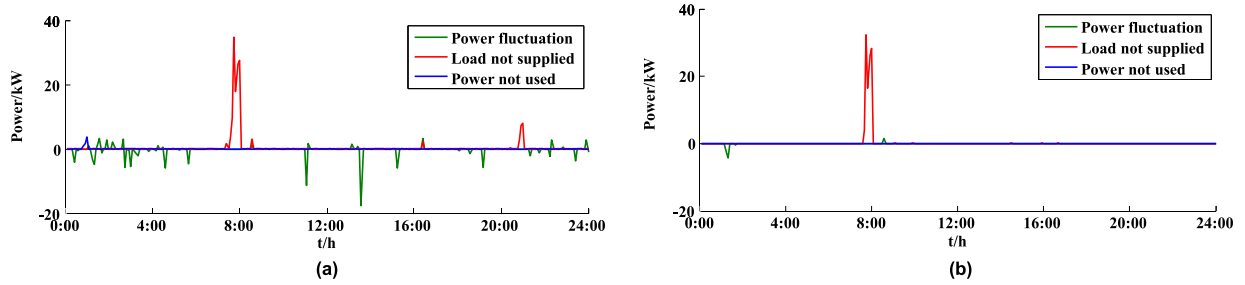

FIGURE 6. Operational performances of the MG in different methods. (a) Traditional method. (b) Proposed method.

2) INFLUENCE OF UNIT FORCED OUTAGE

Figure 7 shows the dispatch results without outage units. The operational costs of the schedule and the dispatch layers are ￥1745.26 and ￥86.00, respectively. The costs decline, compared with the corresponding items in Table 4. Compared with Fig. 5, interchange power with the main grid decreases in Fig. 7, which relieves the impact on the main grid while improving security. The MG can be more dependent

TABLE 6. Results with different predictive precisions.

Fluctuate parameters f				Required Reserve (kWh)		Operation cost (￥)			Operation performance (10^{-4})		
PV	WT	L1	L2	Positive	Negative	Total	Schedule	Dispatch	FOPP	LNSP	PNUP
5%	5%	0%	0%	43.18	42.90	1857.38	1769.86	87.52	14.53	5.84	0.04
10%	5%	5%	5%	101.37	82.25	1890.53	1800.18	90.35	43.70	18.50	0.08
10%	10%	5%	5%	103.83	108.04	1957.43	1811.45	145.98	107.62	29.47	0.29
10%	10%	10%	10%	178.70	196.01	2065.36	1832.17	233.19	307.48	35.66	0.44
15%	15%	10%	10%	197.73	224.77	2096.52	1849.83	246.69	384.29	40.28	0.51

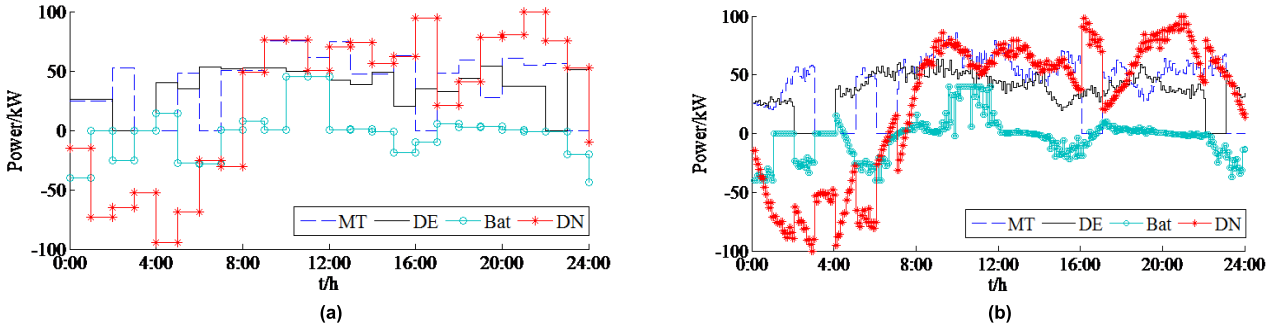

FIGURE 7. Dispatch schemes without outage units. (a) Schedule layer. (b) Dispatch layer.

on the controllable DG units to get enough reserve. If the controllable DG units' forced outage rate is doubled, then the operational costs of the schedule and the dispatch layers are ￥1898.12 and ￥97.24, respectively, which are higher than the corresponding items in Table 4.

TABLE 7. Optimization results with different cost coefficient β_1.

Cost coefficient β_1	Schedule operational cost (￥)	Operation maintenance cost (￥)	SOC cost (￥)	Voltage deviation cost (￥)	Average node voltage deviation (V)
0.5	1800.18	1679.31	0.19	120.68	10.05
1.0	1849.49	1612.12	0.06	237.31	9.89
1.5	1950.95	1600.13	0.03	350.79	9.74
2.0	2079.71	1618.00	0.00	461.71	9.62
2.5	2217.30	1641.90	0.00	575.40	9.59

3) INFLUENCE OF DIFFERENT PENALTY FACTORS

Table 7 shows the optimal scheduling results with different cost coefficients of voltage deviation β_1. The schedule operational cost of the MG accelerates with an increase in β_1. Simultaneously, the average node voltage deviation of the MG decreases with the increase of β_1. Table 8 shows the optimal dispatching results with different cost coefficients of power trace β_3. As shown, the dispatch operational cost increases with the increase of β_3, whereas the power adjustment cost decreases with the increase of β_3. Therefore, the reasonable setting of β_1 and β_3 influences on the reliable and economical operation of the MG.

TABLE 8. Optimization results with different cost coefficient β_3.

Cost Coefficient β_3	Dispatch operational cost (￥)	Operation cost (￥)	Power deviation cost (￥)	Power adjustment cost(￥)	Risk cost (￥)
0.05	180.70	90.35	68.70	16.55	5.1
0.10	178.64	85.62	74.20	14.32	4.5
0.15	183.52	83.13	83.90	13.09	3.4
0.20	187.18	72.81	101.40	10.87	2.1
0.25	190.14	65.23	114.60	9.41	0.9

IV. CONCLUSIONS

To overcome uncertain factors of the MG as the output fluctuation of uncontrollable units, load fluctuation and unit outage, a bi-layer coordinated generation and reserve schedule and dispatch model for a grid-connected MG is proposed to decrease the impact of uncertainties on operational performances. In the upper layer, a day-ahead schedule is created to minimize the operating costs of the MG, and a relaxed reserve configuration with bidirectional boundary constraints is proposed to improve its economy and reliability. In the lower layer, based on the unit outage scenarios, the power output of units is adjusted to follow the real-time fluctuation of the renewables and the load, as well as the accurate reserve configuration is obtained through a successive approximation. The proposed schedule and dispatch framework is more economical and has better operational performance than traditional method with fixed reserve configuration. The influence of MG on the main grid is decreased by autonomous

energy management; hence the proposed model could be used to solve further problems of the grid with high penetration of MGs.

REFERENCES

[1] N. Hatziargyriou, H. Asano, R. Iravani, and C. Marnay, "Microgrids," *IEEE Power Energy Mag.*, vol. 5, no. 4, pp. 78–94, Jul./Aug. 2007.

[2] F. Katiraei, R. Iravani, N. Hatziargyriou, and A. Dimeas, "Microgrids management," *IEEE Power Energy Mag.*, vol. 6, no. 3, pp. 54–65, May/Jun. 2008.

[3] R. H. Lasseter and P. Paigi, "Microgrid: A conceptual solution," in *Proc. IEEE Power Electron. Spec. Conf.*, Aachen, Germany, Jun. 2004, pp. 4285–4291.

[4] S.-J. Ahn, S.-R. Nam, J.-H. Choi, and S.-I. Moon, "Power scheduling of distributed generators for economic and stable operation of a microgrid," *IEEE Trans. Smart Grid*, vol. 4, no. 1, pp. 398–405, Mar. 2013.

[5] A. Khodaei, "Microgrid optimal scheduling with multi-period islanding constraints," *IEEE Trans. Power Syst.*, vol. 29, no. 3, pp. 1383–1392, May 2014.

[6] G. K. Venayagamoorthy, R. K. Sharma, P. K. Gautam, and A. Ahmadi, "Dynamic energy management system for a smart microgrid," *IEEE Trans. Neural Netw. Learn. Syst.*, vol. 27, no. 8, pp. 1643–1656, Aug. 2016.

[7] Y. Cai, T. Huang, E. Bompard, Y. Cao, and Y. Li, "Self-sustainable community of electricity prosumers in the emerging distribution system," *IEEE Trans. Smart Grid*, vol. 8, no. 5, pp. 2207–2216, Sep. 2017.

[8] G. Liu, M. Starke, B. Xiao, and K. Tomsovic, "Robust optimisation-based microgrid scheduling with islanding constraints," *IET Gener., Transmiss. Distrib.*, vol. 11, no. 7, pp. 1820–1828, 2017.

[9] N. Nikmehr and S. Najafi-Ravadanegh, "Optimal operation of distributed generations in micro-grids under uncertainties in load and renewable power generation using heuristic algorithm," *IET Renew. Power Gener.*, vol. 9, no. 8, pp. 982–990, 2015.

[10] A. Gholami, T. Shekari, F. Aminifar, and M. Shahidehpour, "Microgrid scheduling with uncertainty: The quest for resilience," *IEEE Trans. Smart Grid*, vol. 7, no. 6, pp. 2849–2858, Nov. 2016.

[11] H. Wu, M. Shahidehpour, A. Alabdulwahab, and A. Abusorrah, "Thermal generation flexibility with ramping costs and hourly demand response in stochastic security-constrained scheduling of variable energy sources," *IEEE Trans. Power Syst.*, vol. 30, no. 6, pp. 2955–2964, Nov. 2015.

[12] S. Talari, M. Yazdaninejad, and M.-R. Haghifam, "Stochastic-based scheduling of the microgrid operation including wind turbines, photovoltaic cells, energy storages and responsive loads," *IET Gener. Transmiss. Distrib.*, vol. 9, no. 12, pp. 1498–1509, Sep. 2015.

[13] K. Methaprayoon, C. Yingvivatanapong, W.-J. Lee, and J. R. Liao, "An integration of ANN wind power estimation into unit commitment considering the forecasting uncertainty," *IEEE Trans. Ind. Application*, vol. 43, no. 6, pp. 1441–1448, Nov./Dec. 2007.

[14] S. X. Chen and H. B. Gooi, "Sizing of energy storage for microgrids," *IEEE Trans. Smart Grid*, vol. 3, no. 1, pp. 142–151, Mar. 2012.

[15] R. Wang, P. Wang, G. Xiao, and S. Gong, "Power demand and supply management in microgrids with uncertainties of renewable energies," *Int. J. Elect. Power Energy Syst.*, vol. 63, pp. 260–269, Dec. 2014.

[16] H. Liang and W. Zhuang, "Stochastic modeling and optimization in a microgrid: A survey," *Energies*, vol. 7, no. 4, pp. 2027–2050, 2014.

[17] Z. Ding and W.-J. Lee, "A stochastic microgrid operation scheme to balance between system reliability and greenhouse gas emission," *IEEE Trans. Ind. Appl.*, vol. 52, no. 2, pp. 1157–1166, Mar./Apr. 2016.

[18] P. Kou, D. Liang, and L. Gao, "Stochastic energy scheduling in microgrids considering the uncertainties in both supply and demand," *IEEE Syst. J.*, vol. 12, no. 3, pp. 2589–2600, Sep. 2018.

[19] F. Valencia, D. Saez, J. Collado, F. Ávila, A. Marquez, and J. J. Espinosa, "Robust energy management system based on interval fuzzy models," *IEEE Trans. Control Syst. Technol.*, vol. 24, no. 1, pp. 140–157, Jan. 2016.

[20] C. Zhang, Y. Xu, Z. Y. Dong, and J. Ma, "Robust operation of microgrids via two-stage coordinated energy storage and direct load control," *IEEE Trans. Power Syst.*, vol. 32, no. 4, pp. 2858–2868, Jul. 2017.

[21] R. Palma-Behnke *et al.*, "A microgrid energy management system based on the rolling horizon strategy," *IEEE Trans. Smart Grid*, vol. 4, no. 2, pp. 996–1006, Jun. 2013.

[22] H. Wu, X. Liu, and M. Ding, "Dynamic economic dispatch of a microgrid: Mathematical models and solution algorithm," *Int. J. Elect. Power Energy Syst.*, vol. 63, pp. 336–346, Dec. 2014.

[23] Q. Jiang, M. Xue, and G. Geng, "Energy management of microgrid in grid-connected and stand-alone modes," *IEEE Trans. Power Syst.*, vol. 28, no. 3, pp. 3380–3389, Aug. 2013.

[24] Z. Bao, Q. Zhou, Z. Yang, Q. Yang, L. Xu, and T. Wu, "A multi time-scale and multi energy-type coordinated microgrid scheduling solution—Part I: Model and methodology," *IEEE Trans. Power Syst.*, vol. 30, no. 5, pp. 2257–2266, Sep. 2015.

[25] Z. Bao, Q. Zhou, Z. Yang, Q. Yang, L. Xu, and T. Wu, "A multi time-scale and multi energy-type coordinated microgrid scheduling solution—Part II: Optimization algorithm and case studies," *IEEE Trans. Power Syst.*, vol. 30, no. 5, pp. 2267–2277, Sep. 2015.

[26] E. Mayhorn, L. Xie, and K. B. Purry, "Multi-time scale coordination of distributed energy resources in isolated power systems," *IEEE Trans. Smart Grid*, vol. 8, no. 2, pp. 998–1005, Mar. 2017.

[27] Y. Tian, L. Fan, Y. Tang, K. Wang, G. Li, and H. Wang, "A coordinated multi-time scale robust scheduling framework for isolated power system with ESU under high RES penetration," *IEEE Access*, vol. 6, pp. 9774–9784, 2018.

[28] H. Wu *et al.*, "Stochastic multi-timescale power system operations with variable wind generation," *IEEE Trans. Power Syst.*, vol. 32, no. 5, pp. 3325–3337, Sep. 2017.

[29] C. Li *et al.*, "A time-scale adaptive dispatch method for renewable energy power supply systems on islands," *IEEE Trans. Smart Grid*, vol. 7, no. 2, pp. 1069–1078, Mar. 2016.

[30] V. Mohan, J. G. Singh, and W. Ongsakul, "An efficient two stage stochastic optimal energy and reserve management in a microgrid," *Appl. Energy*, vol. 160, pp. 28–38, Dec. 2015.

[31] S. Y. Lee, Y. G. Jin, and Y. T. Yoon, "Determining the optimal reserve capacity in a microgrid with islanded operation," *IEEE Trans. Power Syst.*, vol. 31, no. 2, pp. 1369–1376, Mar. 2016.

[32] G. Liu, M. Starke, B. Xiao, X. Zhang, and K. Tonsovic, "Microgrid optimal scheduling with chance-constrained islanding capability," *Electr. Power Syst. Res.*, vol. 145, pp. 197–206, Apr. 2017.

[33] K. Bruninx, K. van den Bergh, E. Delarue, and W. D'haeseleer, "Optimization and allocation of spinning reserves in a low-carbon framework," *IEEE Trans. Power Syst.*, vol. 31, no. 2, pp. 872–882, Mar. 2016.

[34] A. M. L. da Silva, J. F. da Costa Castro, and R. Billinton, "Probabilistic assessment of spinning reserve via cross-entropy method considering renewable sources and transmission restrictions," *IEEE Trans. Power Syst.*, vol. 33, no. 4, pp. 4574–4582, Jul. 2018.

[35] E. Bompard *et al.*, "A multi-site real-time co-simulation platform for the testing of control strategies of distributed storage and V2G in distribution networks," in *Proc. EPE ECCE Europe*, Karlsruhe, Germany, Sep. 2016, pp. 1–9.

[36] J. Zhang *et al.*, "A bi-level program for the planning of an islanded microgrid including CAES," *IEEE Trans. Ind. Appl.*, vol. 52, no. 4, pp. 2768–2777, Jul./Aug. 2016.

[37] R. Doherty and M. O'Malley, "A new approach to quantify reserve demand in systems with significant installed wind capacity," *IEEE Trans. Power Syst.*, vol. 20, no. 2, pp. 587–595, May 2005.

[38] M. D. Ilic, "From hierarchical to open access electric power systems," *Proc. IEEE*, vol. 95, no. 5, pp. 1060–1084, May 2007.

[39] C.-F. Juang, "A hybrid of genetic algorithm and particle swarm optimization for recurrent network design," *IEEE Trans. Syst., Man, Cybern. B, Cybern.*, vol. 34, no. 2, pp. 997–1006, Apr. 2004.

[40] A. A. Moghaddam, A. Seifi, and T. Niknam, "Multi-operation management of a typical micro-grids using particle swarm optimization: A comparative study," *Renew. Sustain. Energy Rev.*, vol. 16, no. 2, pp. 1268–1281, 2012.

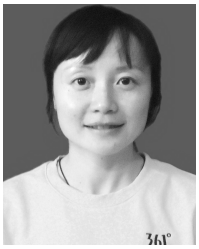

XIA LEI received the B.Sc. and M.Sc. degrees in electrical engineering from Sichuan University. She is currently a Professor with the School of Electrical Engineering and Electronic Information, Xihua University. Her research interest includes the optimal operation of electrical systems with renewable energy and power markets.

TAO HUANG received the Ph.D. degree from the Politecnico di Torino, Turin, Italy. He is currently with the Department of Energy, Politecnico di Torino, and with the School of Electrical Engineering and Electronic Information, Xihua University. His research interests include critical infrastructure protection, vulnerability detection and resilience enhancement, electricity markets, and smart grids.

YONG FANG received the B.Sc. and M.Sc. degrees in electrical engineering from Sichuan University. He is currently a Lecturer with Xihua University. His research interest includes the operation analysis of electrical systems.

YI YANG received the M.Sc. degree in electrical engineering from Xihua University. He is currently with Bazhong Electrical Company. His main research interest includes the optimal dispatch of microgrid.

PENG WANG received the Ph.D. degree from the University of Saskatchewan, Canada. He is currently a Professor with the Electrical and Electronic Engineering School, Nanyang Technological University, Singapore. His research interests include power system planning and operation, renewable energy planning, solar/electricity conversion systems, power market, and power system reliability analysis.